

1  
2  
3  
4  
5  
6  
7  
8  
9  
10  
11  
12  
13  
14  
15  
16  
17  
18  
19  
20  
21  
22  
23  
24  
25  
26

**Technical Note:**

**Multi-year Changes in the Brewer-Dobson Circulation from HALOE Methane**

Ellis Remsberg

Science Directorate, NASA Langley Research Center, 21 Langley Blvd.,

Mail Stop 401B, Hampton, Virginia, 23681, USA

Correspondence: Ellis Remsberg (ellis.e.remsberg@nasa.gov)

November, 2023

**Abstract.** This study makes use of Halogen Occultation Experiment (HALOE) methane (CH<sub>4</sub>) in a search for multi-year changes in the Brewer-Dobson Circulation (BDC). Changes in CH<sub>4</sub> are determined for three, successive 5-yr time spans from 1992 to 2005, and there are significant differences in them. There is a clear separation for the changes in the northern hemisphere near 30 hPa or at the transition of the shallow and deep branches of the BDC. The CH<sub>4</sub> changes are positive and large in the shallow branch following the eruption of Pinatubo, but they then decrease and agree with tropospheric trends in the late 1990s and early 2000s. CH<sub>4</sub> decreases in the upper part of the deep branch from 1992 to 1997 or following the eruption of Pinatubo. CH<sub>4</sub> continues to decrease in the deep branch in the late 1990s but then increases in the early 2000s, although those changes are small compared with the seasonal and interannual variations of CH<sub>4</sub>. Multi-year changes are due, in part, to wave forcings during El Nino Southern Oscillation (ENSO) of 1997-1998 and beyond and to episodic, sudden stratospheric warming (SSW) events during both time spans. It is concluded that time series of HALOE CH<sub>4</sub> provide effective tracer diagnostics for studies of the nature of the BDC from 1992 to 2005.

27

## 28 **1. Introduction**

29 Global-scale stratospheric transport is characterized in each hemisphere by a seasonal Brewer-  
30 Dobson circulation (BDC), consisting of upward transport in the tropics, poleward transport to  
31 higher latitudes, and descent in the polar vortex region (e.g., Butchart, 2014). Model studies  
32 indicate that there are also multi-year changes in the BDC in response to increases in the  
33 greenhouse gases (GHG) and to dynamical forcings during El Nino/Southern Oscillation  
34 (ENSO) events, but where the effects of those forcings may differ within the shallow (lower) and  
35 deep (upper) regions of the BDC. Remsberg (2015) reported that the distributions of methane  
36 ( $\text{CH}_4$ ) from the Halogen Occultation Experiment (HALOE) provide tracer diagnostics for  
37 changes in the BDC. The present study is a refinement of his initial analysis and gives some  
38 insight on mechanisms for changes in the BDC. Section 2 is a brief description of the methane  
39 data and the analysis approach for them. Section 3 presents the results of the analyses in terms  
40 of changes in the distribution of  $\text{CH}_4$  for three successive 5-yr time spans. Qualitative  
41 attributions are also considered for those changes. Section 4 summarizes the findings from this  
42 exploratory study.

43

## 44 **2. Data and Analysis Method**

45 HALOE obtained sunrise (SR) and sunset (SS) occultation measurements across latitude zones  
46 throughout its mission of October 1991 to November 2005. The present study considers zonal  
47 averages of  $\text{CH}_4$  for nine latitude zones and at twelve pressure levels (0.4 to 50 hPa), for a total  
48 of 108 separate time series. A minimum of 5 profiles gives representative zonal averages for  
49 each latitude zone; averages are based on many more profiles in most instances. Figure 1 shows  
50 example time series from zonal averages of the SR and SS measurements at specific pressure  
51 levels and in three different latitude zones. Figure 1(a) is the time series for the 10 hPa level at  
52  $30^\circ\text{N}$  latitude, and there is a clear quasi-biennial oscillation (QBO) signal in the data. Figure  
53 1(b) is for 10 hPa at  $30^\circ\text{S}$ , where there is a combination of annual (AO), semi-annual (SAO), and  
54 QBO signals. One can also see that seasonal and interannual variations are much larger than the

55 longer-term changes. Figure 1(c) is for 2 hPa at 45°N, where CH<sub>4</sub> decreases gradually in the  
56 early to middle 1990s but where it also has large amplitudes in early 2002 and 2004.

57

58 The analysis of CH<sub>4</sub> for this study is in the manner of Remsberg (2015) with the following  
59 modifications. The nine latitude zones are from 60°S to 60°N with a spacing of 15° and no  
60 overlap. The latitude bins are a bit narrower than before (15° versus 20°) but still provide  
61 representative sampling, even at ±45° latitude from 2000 to 2005 when the samples from  
62 HALOE are limited. To look for secular trends in CH<sub>4</sub>, multiple linear regression (MLR)  
63 analysis was applied to the CH<sub>4</sub> time series, as separated into three, 5-yr time spans that overlap  
64 by one year (July 1992 to June 1997; July 1996 to June 2001; and July 2000 to June 2005). The  
65 beginning and end months of July and June, respectively, were selected to avoid large excursions  
66 in CH<sub>4</sub> at the end points of time series for the northern hemisphere during the dynamically active  
67 winter season. Data prior to July 1992 were not used, to avoid issues related to variable solar  
68 lock-down procedures for the HALOE sun sensor and because of significant extinction from  
69 interfering aerosols following the Pinatubo eruption of June 1991. The analyses also do not  
70 include the period after June 2005, when HALOE operations were limited.

71

72 An initial MLR analysis was applied to the 13-yr time span of the HALOE measurements for a  
73 range of pressures and latitudes but using only AO and SAO terms. Time series residuals from  
74 those runs were analyzed for interannual cycles, yielding significant terms with periods of 882  
75 days (~29-month or QBO-like) and of 690 days (22.6-month or sub-biennial (SB)). Those two  
76 terms were highly significant for many of the latitude/pressure time series, so they were included  
77 along with the seasonal terms for the MLR model. The 5-yr (or 60 month) time span is  
78 equivalent to two complete QBO cycles and avoids biases in the MLR trends due to that periodic  
79 term. A biennial (718-dy) term was also indicated for the subtropics, but it was not uniformly  
80 present elsewhere and was not retained for the model. A linear term completes the final MLR  
81 model; the analyses also correct for lag-1 autoregressive (AR1) effects. The MLR model fit to  
82 the data points is shown by the oscillating solid curve for July 1996 to June 2001 in each panel of  
83 Fig. 1, and the combination of the constant and linear terms is the dashed line. One can see that  
84 the seasonal and interannual variations have large amplitudes compared with the overall 5-yr

85 trend line, such that even minor changes from year to year can affect the linear changes.  
86 Although the MLR fits and trends are based on analyzed AR1 values for each case, the MLR  
87 curves in Fig. 1 are based on  $AR1 = 0$  and give maximum amplitudes for the periodic terms.

88

89 The sensitivity of the trend coefficient to the approximate QBO term of the MLR fit was  
90 determined for Fig. 1(a) ( $30^{\circ}N$ , 10 hPa), where a QBO cycle shows clearly. Specifically, the  
91 length of the QBO cycle was altered (28 months versus 29.5 months) as well as the length of the  
92 time span for the MLR analysis (58 months rather than 60 months). The resulting trend  
93 coefficients in each case differ by less than 6% from the one of Fig. 1(a). Figure 1(c) focuses on  
94 the upper stratosphere, where  $CH_4$  decreases from 1992 to 1997 or from one year after the  
95 Pinatubo eruption. The 5-yr trend is less negative from 1996 to 2001 and then is positive from  
96 2000 to 2005, punctuated by two winter maximums in early 2002 and 2004.

97

98 The distribution of the average  $CH_4$  (its constant term) is shown in Figure 2 for the time span of  
99 July 1996 to June 2001. Tropical entry-level values extend upward and are transported poleward  
100 in each hemisphere.  $CH_4$  decreases with altitude and latitude, due to the relatively slow chemical  
101 conversion of  $CH_4$  to water vapor ( $H_2O$ ) and molecular hydrogen ( $H_2$ ) in the upper stratosphere  
102 (Brasseur and Solomon, 2005). That decay of  $CH_4$  is nearly symmetric between the two  
103 hemispheres. The primary purpose of Fig. 2 is to show the vertical and meridional gradients of  
104  $CH_4$  that are acted upon by the BDC, generically considered as hemispheric, net circulations  
105 composed of tropical ascent, poleward transport, plus descent in the polar vortex region.  
106 Although the  $CH_4$  distributions for the other two 5-yr time spans are like that of Fig. 2, there are  
107 small but distinct differences in the 5-yr changes in  $CH_4$  for the three successive time spans.

108

109 Distributions of the linear terms (% change / 5-yr) from the zonally averaged  $CH_4$  data are shown  
110 and discussed in Section 3 for each of the three periods of July 1992 to June 1997, July 1996 to  
111 June 2001, and July 2000 to June 2005. Notably, there is good continuity for the trends with  
112 pressure and latitude, indicating that each distribution is meaningful and related physically to  
113 multi-year changes for the large-scale BDC. Mechanisms giving rise to the changing  $CH_4$  are

114 related to external (volcanic) and/or wave forcings followed by radiative and/or chemical  
115 relaxations therefrom. The changes in CH<sub>4</sub> are also compared with estimates of the stratospheric  
116 net circulation that have been diagnosed and reported by other researchers.

117

### 118 **3. Multi-year changes in CH<sub>4</sub>**

#### 119 *(a) July 1992 to June 1997*

120 Figure 3 shows that CH<sub>4</sub> decreased in the upper stratosphere and lower mesosphere from July  
121 1992 to June 1997 or from one year after the Pinatubo eruption of June 1991. The shading  
122 indicates where the trends are robust, the dark shading having a confidence interval (CI) of  
123 greater than 90% and the light shading having CI between 70 and 90%. Note that there are  
124 small, positive trends in CH<sub>4</sub> within the lower stratosphere, due to its tropospheric trends of ~0.4  
125 % / yr (or 2.0 % for this 5-yr period) (Dlugokencky et al., 2009). Changes of the CH<sub>4</sub>  
126 distributions across the 5-yr time span represent where there were accelerations of the BDC  
127 (positive changes of greater than the tropospheric trends of ~2.0 %) or decelerations of the BDC  
128 (changes of less than ~2.0 %).

129

130 Negative changes in CH<sub>4</sub> in the upper regions of Fig. 3 imply that there was an overall  
131 weakening of the deep branch (above the ~20-hPa level) of the stratospheric BDC during this 5-  
132 yr period. Those negative changes are more pronounced at middle latitudes of the northern than  
133 of the southern hemisphere, indicating that there was ascent of CH<sub>4</sub> within the deep branch of the  
134 BDC in the northern subtropics due to external forcings from the Pinatubo eruption near 15°N  
135 followed by a relaxation toward lower values thereafter. In fact, separate, zonal mean cross  
136 sections of HALOE CH<sub>4</sub> (not shown) reveal that the 0.8 ppmv contour of CH<sub>4</sub> occurred at ~4  
137 hPa in November 1991 but had risen to ~2 hPa by February 1992, most likely a response of the  
138 BDC to winter wave forcings (e.g., Russell et al. 1999). Thereafter, the CH<sub>4</sub> values that had  
139 been lofted to higher altitudes underwent a gradual decline over time. Sudden stratospheric  
140 warming (SSW) events also tend to accelerate the deep branch of the BDC and mix middle  
141 latitude and polar air; that mixing flattens the contours of zonal average CH<sub>4</sub> mixing ratio.

142 However, there were no SSW events in the northern hemisphere during 1992 to 1997 (Choi et  
143 al., 2019).

144

145 A more traditional indicator of changes in the BDC is stratospheric age-of-air (AoA), where  
146 negative AoA indicates acceleration and positive AoA implies a deceleration of the BDC.  
147 Pitari et al. (2016) estimated that AoA decreased in the middle to upper stratosphere by ~0.5 to  
148 0.7 yr during 1991-1992, due mainly to ascent following the eruption of Pinatubo. Fig. 3  
149 indicates a decline of CH<sub>4</sub> (and presumably an increase in AoA) from July 1992 onward.  
150 Methane is not a perfect tracer, however, as it has a chemical lifetime as short as only a few  
151 months at 45 km (~1.5 hPa) and then lengthening to 6 months and longer at 55 km and above  
152 and at 40 km and below (Brasseur and Solomon, 2005). The relatively short lifetime of CH<sub>4</sub> at  
153 1.5 hPa means that even the seasonal variations of CH<sub>4</sub> are dampened at that level. The near-  
154 zero changes for CH<sub>4</sub> near 15°S and 2 hPa in Fig. 3 may imply that there was still some transport  
155 of CH<sub>4</sub> to that region from the tropics after July 1992.

156

157 The 5-yr changes in Fig. 3 also indicate that there was an accumulation of CH<sub>4</sub> at ~20 to 30 hPa  
158 at middle latitudes of both hemispheres during this period, in reasonable accord with a net  
159 poleward transport of tropical CH<sub>4</sub> at the top of the shallow (below the ~20-hPa level) branch of  
160 the BDC. The tropical trend of 3 to 4 % at 20 to 30 hPa is half that at middle latitudes (8 %),  
161 although it is still larger than the tropospheric trends for CH<sub>4</sub> of ~2.0 % for this 5-yr period.

162

163 Figure 4 gives more detail about the effects of the Pinatubo eruption on CH<sub>4</sub> in the lower  
164 stratosphere. Fig. 4(a) is for 15°N, 50 hPa and shows an initial increase in CH<sub>4</sub> in 1991 to the  
165 middle of 1992, followed by decreasing values through 1993. HALOE CH<sub>4</sub> values are of the  
166 order of 1.55 ppmv in 1992, declining to 1.45 ppmv in 1993, and then increasing again.  
167 Independent CH<sub>4</sub> measurements at ground level are between 1.70 and 1.75 ppmv (Dlugokencky  
168 et al., 2009). As an aside, HALOE CH<sub>4</sub> values for SR in Fig. 4(a) are consistently larger than for  
169 SS. Those differences are likely due to uncorrected detector hysteresis effects for tropical SR  
170 measurements just above cloud tops; they decrease at 30 hPa and are negligible at 20 hPa. Diallo

171 et al. (2017) reported that AoA decreased during the first six months following the eruption of  
172 Pinatubo due to tropical upwelling. Then, AoA increased from early 1992 to spring 1993  
173 between 20°S and 30°N and from 20 to 27 km (~50 hPa to 15 hPa), implying a deceleration of  
174 the shallow branch of the BDC during that time. The HALOE SR and SS CH<sub>4</sub> variations are in  
175 accord with the changes in AoA from 1991 to 1993 in the shallow branch of the BDC.

176  
177 Figure 4(b) is the HALOE CH<sub>4</sub> time series for 45°N, 30 hPa, and it shows a gradual increase of  
178 CH<sub>4</sub> for 1993 to 1997. Yet, Diallo et al. (2017) reported increases in AoA for 1993 at tropical  
179 and middle latitudes due to meridional mixing, followed by decreases in mixing and AoA  
180 through 1997. Fig. 3 suggests that there was an accumulation of CH<sub>4</sub> at middle latitudes between  
181 ~20 and 30 hPa, due in part to that mixing trend. It may also be that there was an overall  
182 slowdown in the BDC during this 5-yr period, which was absent of SSW events and any  
183 enhanced descent of CH<sub>4</sub>-poor, polar air plus its subsequent mixing to middle latitudes.

184

185 *(b) July 1996 to June 2001*

186 Figure 5 shows the 5-yr CH<sub>4</sub> changes for 1996 to 2001, when there were several SSW events—  
187 on 15 December 1998, 25 February 1999, and 20 March 2000 (Choi et al., 2019). The negative  
188 trends in the upper stratosphere are smaller in the northern hemisphere and larger in the southern  
189 hemisphere than in Fig. 3, suggesting that there was tropical ascent but also increased mixing of  
190 CH<sub>4</sub> to higher latitudes, related in part to SSW activity. Those changes are also where the  
191 chemical loss of CH<sub>4</sub> to H<sub>2</sub>O and H<sub>2</sub> may be a factor. It is apparent that there was greater  
192 meridional transport of CH<sub>4</sub> from the tropics to middle latitudes and an accumulation of CH<sub>4</sub> at  
193 ~10 hPa in both hemispheres during 1996 to 2001. Those positive trends are at a level of the  
194 stratosphere where the conversion of CH<sub>4</sub> to H<sub>2</sub>O and H<sub>2</sub> is not as effective.

195

196 There was a major warm ENSO event in 1997-1998 that altered wave forcing effects on CH<sub>4</sub> and  
197 for the BDC. Randel et al. (2009) and Calvo et al. (2010) reported enhanced upwelling in the  
198 tropics and an acceleration of the BDC at that time. Diallo et al. (2019) reported that ENSO

199 leads to the overall strengthening of the shallow branch of the BDC in the extratropics. It may  
200 be that enhanced poleward transport in the shallow branch is why the CH<sub>4</sub> changes are more  
201 nearly zero in the tropics and agree closely with tropospheric trends that were smaller after 1995  
202 (or ~1.0 % / 5-yr) (Dlugokencky et al., 2009). There is a clear separation at ~30 hPa in the sign  
203 of the changes in the shallow versus the deep branch of the BDC in the northern hemisphere.

204

205 The 1997-1998 warm ENSO event occurred near solar minimum, for which Calvo and Marsh  
206 (2011) also found enhanced wave forcing in the middle and upper stratosphere. That activity  
207 leads to acceleration of the BDC and poleward transport of CH<sub>4</sub> to the extratropics. Barriopedro  
208 and Calvo (2014) also found connections between ENSO and SSW events, although the exact  
209 effects depend on the relative sequence of those events. Since major SSWs within 1996-2001  
210 occur in December 1998, February 1999 and in March 2000, it is likely that they merely led to  
211 further accelerations of the BDC. As an example, Tao et al. (2015) gave details about how the  
212 SSW of 2009 led to an acceleration of the BDC. Their analyses may support the present finding  
213 of increases in CH<sub>4</sub> in the extratropics near 10 hPa in Fig. 5. However, more focused studies of  
214 the relative roles of SSWs and ENSO on the results of Fig. 5 are beyond the scope of the present  
215 exploratory study.

216

217 *(c) July 2000 to June 2005*

218 There was even more SSW activity in the northern hemisphere during the 5-yr span from 2000 to  
219 2005 (on 11 February 2001, 2 January 2002, 18 January 2003, and 7 January 2004, according to  
220 Choi et al., 2019). The distribution of changes in CH<sub>4</sub> in Figure 6 includes the net effect of those  
221 episodic SSW events. There was an increase in CH<sub>4</sub> at upper altitudes, where the effect of SSWs  
222 may have also led to greater poleward transport of CH<sub>4</sub> to higher latitudes. As before, an SSW  
223 event accelerates the deep branch of the BDC, bringing more CH<sub>4</sub> to high altitudes and greater  
224 meridional transport to higher latitudes. At the stratopause (~1 hPa) and in the lower mesosphere  
225 even small changes in CH<sub>4</sub> mixing ratio translate to relatively large percentage changes. Those  
226 changes are from negative to positive from Fig. 5 to Fig. 6 and are rather uniform across latitude.  
227 On the other hand, the changes near 10 hPa and at middle latitudes of the northern hemisphere



228 are weaker now than in Fig. 5. Fig. 1(a) indicates that this change may be a consequence, in part,  
229 of large seasonal amplitudes for CH<sub>4</sub> in early 2001 and in 2005 or near the end points of the 5-yr  
230 period from July 2000 to June 2005.

231

232 In the southern hemisphere there was an anomalous SSW event on 22 September 2002, leading  
233 to a splitting of the polar vortex (Newman and Nash, 2005). The CH<sub>4</sub> changes from Fig. 5 to  
234 Fig. 6 at 10 hPa and 30°S were likely altered by that event (c.f., the time series segments in Fig.  
235 1(b) for those two 5-yr periods). Note that there is no clear separation of the shallow and deep  
236 branches of the BDC for the southern hemisphere in Fig. 6.

237

238 Figure 7 provides a clearer picture of what occurred from 2000 to 2005. Fig. 7(a) is a time series  
239 of CH<sub>4</sub> at 45°S and 20 hPa, and it shows pronounced annual cycles in CH<sub>4</sub>. A peak seasonal  
240 value occurs in 2001, and it may be influencing the overall analyzed trend for that time span. On  
241 the other hand, there is little indication of a change in CH<sub>4</sub> at the time of the anomalous SSW  
242 event of September 2002. Fig. 7(b) shows the corresponding CH<sub>4</sub> time series at the Equator and  
243 20 hPa, where CH<sub>4</sub> variations are forced primarily by the QBO. There is a clear decrease in CH<sub>4</sub>  
244 in 2001 compared to the maximum at 45°S in Fig. 7(a). Fig. 7(b) also shows that tropical QBO  
245 signals are nearly absent in CH<sub>4</sub> from 1996 to 2000. Bönisch et al. (2011) reported that tropical  
246 upwelling increased after 2000 and accelerated the shallow branch of the BDC. Similar studies  
247 based on variations in CH<sub>4</sub> may be helpful in determining the nature of the shallow layer of the  
248 BDC both prior to and after 2000.

249

#### 250 **4. Summary findings**

251 The present study is an analysis of the distributions of HALOE CH<sub>4</sub> for indications of secular  
252 changes in the BDC. Linear trends in CH<sub>4</sub> were determined for three, successive 5-yr time  
253 spans, and there are significant differences between them. There is a clear separation of the deep  
254 and shallow branches of the BDC at about 30 hPa in the northern hemisphere in each time span.  
255 Although the changes for CH<sub>4</sub> in the shallow branch are rather large following the eruption of

256 Pinatubo, they agree well with tropospheric trends for CH<sub>4</sub> during the late 1990s and early  
257 2000s. There are decreasing changes in the upper part of the deep branch of the BDC in the  
258 early to middle 1990s, indicating a decline of CH<sub>4</sub> from one year after the eruption. CH<sub>4</sub>  
259 changes in the middle and upper stratosphere differ markedly for the early 2000s compared to  
260 those of the late 1990s, although those differences are small compared to the seasonal and  
261 interannual variations of CH<sub>4</sub>. In addition, the seasonal changes within the deep branches differ  
262 in each hemisphere, perhaps due to episodic SSW events and to wave forcings during ENSO.

263

264 In terms of multi-year changes for the BDC, it appears that during the period of 1992 to 1997  
265 there was acceleration of the shallow branch and deceleration of the deep branch. However,  
266 those implied changes in the BDC may be anomalous because of the large perturbation to the  
267 CH<sub>4</sub> distribution in 1991 from the Pinatubo eruption. During 1996 to 2001 the changes in the  
268 shallow branch were nearer to zero, while decreasing trends persisted in the deep branch. Yet, it  
269 also appears that there was acceleration of the poleward transport and mixing at middle latitudes  
270 within the layer from ~30 hPa to ~7 hPa during that 5-yr period. Then, there was a deceleration  
271 in the shallow branch and acceleration in the deep branch of the BDC during 2000 to 2005. The  
272 implied BDC also differed markedly in the two hemispheres over that final 5-yr span. It is  
273 concluded that time series of HALOE CH<sub>4</sub> provide effective tracer diagnostics for studies of the  
274 secular nature of the BDC from 1992 to 2005.

275

276 *Data availability.* The HALOE V19 profiles are at the NASA EARTHDATA site of EOSDIS,  
277 and its website is [https://disc.gsfc.nasa.gov/datacollection/UARHA2FN\\_019.html](https://disc.gsfc.nasa.gov/datacollection/UARHA2FN_019.html) (Russell et al.,  
278 1999).

279

280 *Competing interests.* The author has declared that there are no competing interests.

281

282 *Acknowledgements.* The author carried out this work while serving as a Distinguished Research  
283 Associate of the Science Directorate at NASA Langley. He thanks Larry Gordley for alerting  
284 him of possible detector hysteresis effects for the CH<sub>4</sub> gas filter correlation channel of HALOE.

285

## 286 **References**

287 Barriopedro, D., and Calvo, N.: On the Relationship between ENSO, Stratospheric Sudden  
288 Warmings, and Blocking, *J. Climate*, 27, 4704-4720, <https://doi.org/10.1175/JCLI-D-1300770.1>,  
289 2014.

290

291 Bönisch, H., Engel, A., Birner, T., Hoor, P., Tarasick, D. W., and Ray, E. A.: On the structural  
292 changes in the Brewer-Dobson circulation after 2000, *Atmos. Chem. Phys.*, 11, 3937–3948,  
293 <https://doi.org/10.5194/acp-11-3937-2011>, 2011.

294

295 Brasseur, G. and Solomon, S.: *Aeronomy of the Middle Atmosphere: Chemistry and Physics of*  
296 *the Stratosphere and Mesosphere*, Dordrecht: Springer, 3rd Edition, 2005.

297

298 Butchart, N.: The Brewer-Dobson Circulation, *Rev. Geophys.*, 52, 157-184,  
299 <https://doi.org/10.1002/2013RG000448>, 2014.

300

301 Calvo, N., and Marsh, D. R.: The combined effects of ENSO and the 11-year solar cycle on the  
302 Northern Hemisphere polar stratosphere, *J. Geophys. Res.*, 116, D23112,  
303 <https://doi.org/10.1029/2010JD015226> . 2011.

304

305 Calvo, N., Garcia, R. R., Randel, W. J., and Marsh, D. R.: Dynamical Mechanism for the  
306 Increase in Tropical Upwelling in the Lowermost Tropical Stratosphere during Warm ENSO  
307 Events, *J. Atmos. Sci.*, 67, 2331-2340, <https://doi.org/10.1175/2010JAS3433.1>, 2010.

308

309 Choi, H., Kim, B-M., and Choi, W.: Type Classification of Sudden Stratospheric Warming  
310 Based on Pre- and Postwarming Periods, *J. Climate*, 32, 2349-2367,  
311 <https://doi.org/10.1175/JCLI-D-18-0223.1>, 2019.

312

313 Diallo, M., Konopka, P., Santee, M. L., Müller, R., Tao, M., Walker, K. A., Legras, B., Riese,  
314 M., Ern, M., and Ploeger, F.: Structural changes in the shallow and transition branch of the  
315 Brewer–Dobson circulation induced by El Niño, *Atmos. Chem. Phys.*, 19, 425–446,  
316 <https://doi.org/10.5194/acp-19-425-2019>, 2019.

317

318 Diallo, M., Ploeger, F., Konopka, P., Birner, T., Müller, R., Riese, M., Garny, H., Legras,  
319 B., Ray, E., Berthet, G., and Jegou, F.: Significant contributions of volcanic aerosols to decadal  
320 changes in the stratospheric circulation, *Geophys. Res. Lett.*, 12, 10780–10791,  
321 <https://doi.org/10.1002/2017GL074662>, 2017.

322

323 Dlugokencky, E. J., Bruhwiler, L., White, J. W. C., Emmons, L. K., Novelli, P. C., Montzka, S.  
324 A., Masarie, K. A., Lang, P. M., Crotwell, A. M., Miller, J. B., and Gatti, L. V.: Observational  
325 constraints on recent increases in the atmospheric CH<sub>4</sub> burden, *Geophys. Res. Lett.*, 36, L18803,  
326 <https://doi.org/10.1029/2009GL039780>, 2009.

327

328 Newman, P. A., and Nash, E. R.: The Unusual Southern Hemisphere Stratosphere Winter of  
329 2002, *J. Atmos. Sci.*, 62, 614-628, <https://doi.org/10.1175/JAS-3323.1>, 2005.

330

331 Pitari, G., Cionni, I., Di Genova, G., Visioni, D., Gandolfi, I., and Mancini, E.: Impact of  
332 Stratospheric Volcanic Aerosols on Age-of-Air and Transport of Long-Lived Species,  
333 *Atmosphere*, 7, 149, <https://doi.org/10.3390/atmos7110149>, 2016.

334

335 Randel, W. J., Garcia, R. R., Calvo, N., and Marsh, D. R.: ENSO influence on zonal mean  
336 temperature and ozone in the tropical lower stratosphere, *Geophys. Res. Lett.*, 36, L15822,  
337 <https://doi.org/10.1029/2009GL039343>, 2009.

338

339 Remsberg, E.: Methane as a diagnostic tracer of changes in the Brewer-Dobson circulation of the  
340 stratosphere, *Atmos. Chem. Phys.*, 15, 3739–3754, <https://doi.org/10.5194/acp-15-3739-2015>,  
341 2015.

342

343 Russell III, J. M., et al.: UARS Halogen Occultation Experiment (HALOE) Level 2 V019,  
344 Greenbelt, MD, USA, Goddard Earth Sciences Data and Information Services Center (GES  
345 DISC) [data set], [https://disc.gsfc.nasa.gov/datacollection/UARHA2FN\\_019.html](https://disc.gsfc.nasa.gov/datacollection/UARHA2FN_019.html) (last access:  
346 23 August 2023), 1999.

347

348 Tao, M., Konopka, P., Ploeger, F., Groß, J.-U., Müller, R., Volk, C., Walker, K., and  
349 Riese, M.: Impact of the 2009 major stratospheric sudden warming on the composition of the  
350 stratosphere, *Atmos. Chem. Phys.*, pp. 8695–8715, <https://doi.org/10.5194/acp-15-8695-2015>,  
351 2015.

352

353

354

355

356

357

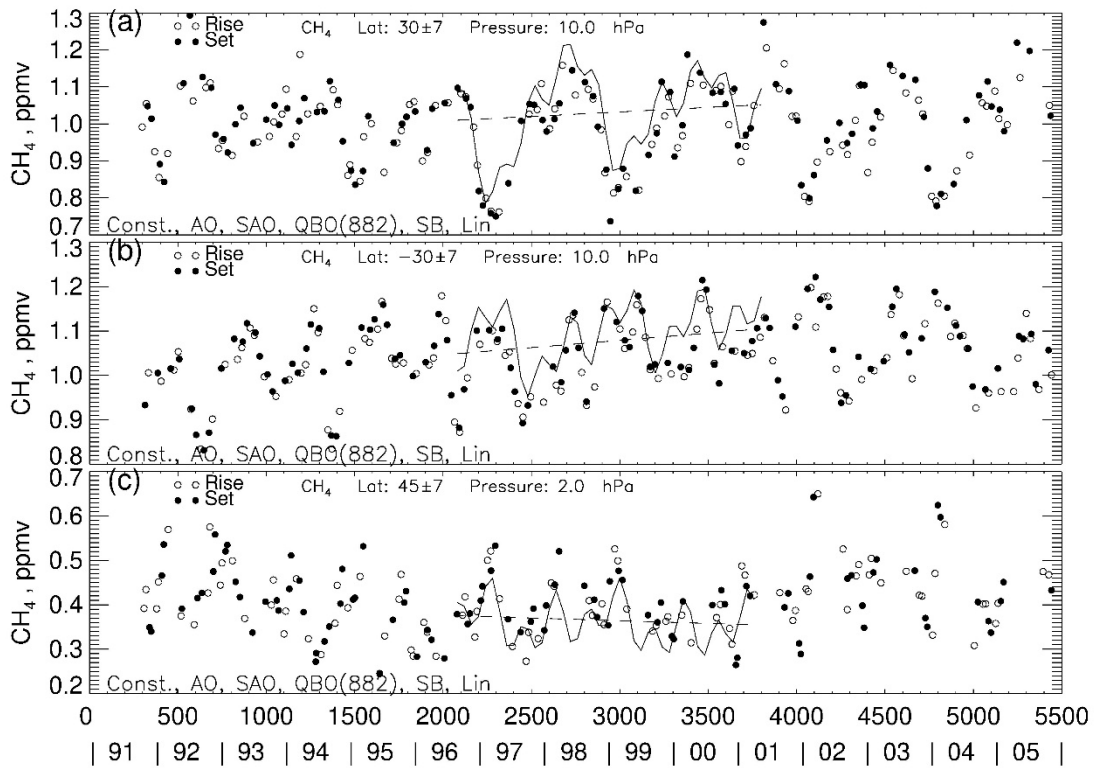
358

359

360

361 **Figures**

362



363

364 Figure 1—Time series of HALOE CH<sub>4</sub> (a) 30°N and 10 hPa, (b) 30°S and 10 hPa, and (c) 45°N  
365 and 2 hPa. MLR fit for July 1996 through June 2001 is the solid curve, and its linear trend is the  
366 dashed line. Day numbers on the abscissa are from 1 January 1991. Model terms are listed at  
367 bottom left. The Pinatubo eruption occurred in June 1991.

368

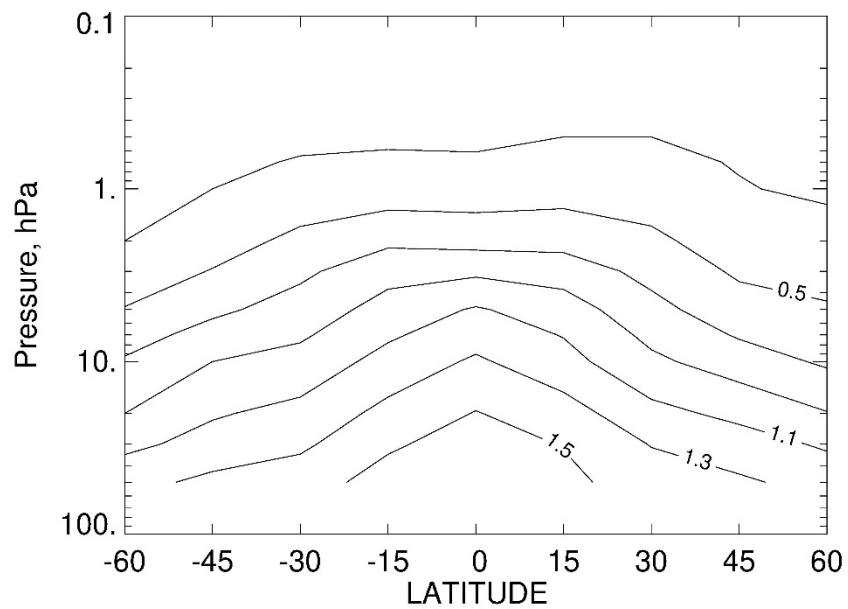
369

370

371

372

373



374

375 Figure 2—Average CH<sub>4</sub> for July 1996 through June 2001; contour interval is 0.2 ppmv.

376

377

378

379

380

381

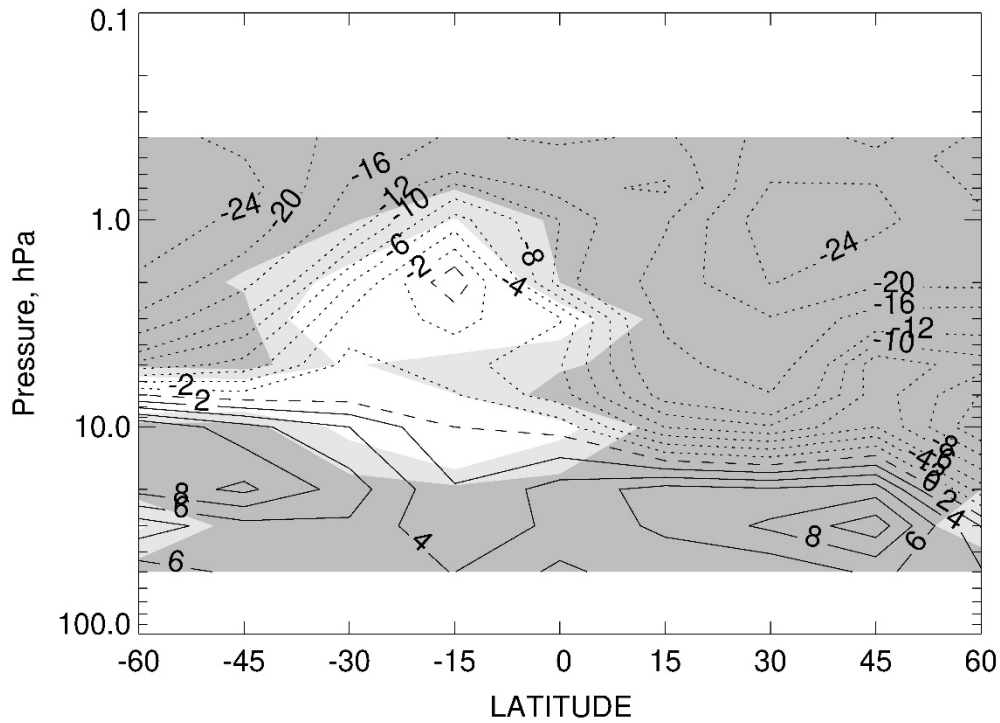
382

383

384

385

386



388

389

390 Figure 3—Changes in CH<sub>4</sub> for July 1992 through June 1997 (in % / 5-yr); positive changes are  
 391 solid, negative changes are dotted, and zero is dashed. Contour interval is 2 % within ±12 % but  
 392 4 % outside that range. Dark shading shows where the confidence interval (CI) for the trends is  
 393 greater than 90 %, and light shading shows where CI is between 70 and 90 %.

394

395

396

397

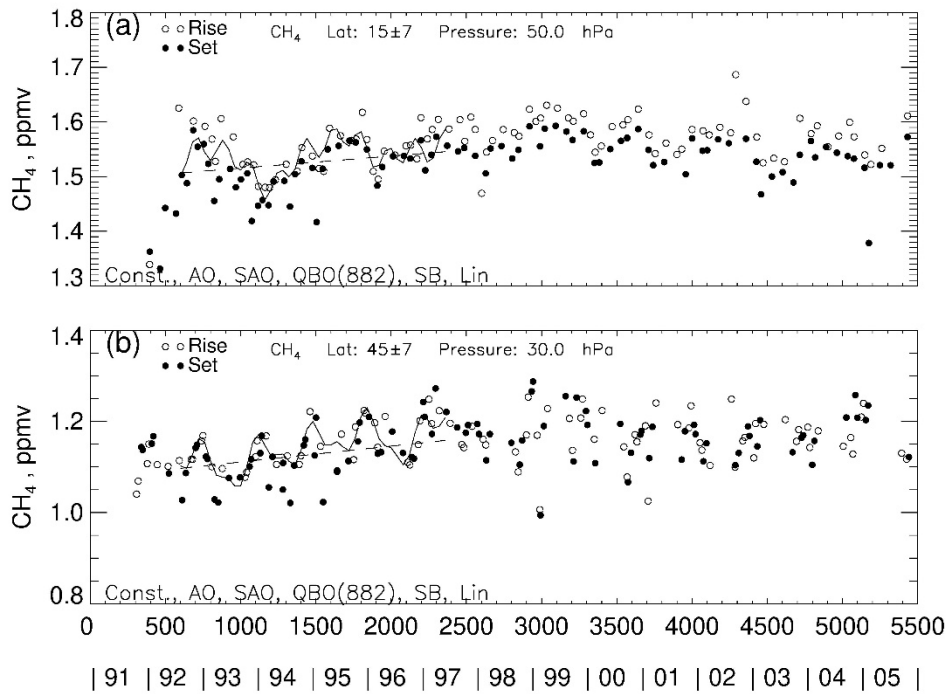
398

399

400



401



402

403

404 Figure 4—As in Fig. 1, but 4(a) is for 15°N and 50 hPa, and 4(b) is for 45°N and 30 hPa.

405

406

407

408

409

410

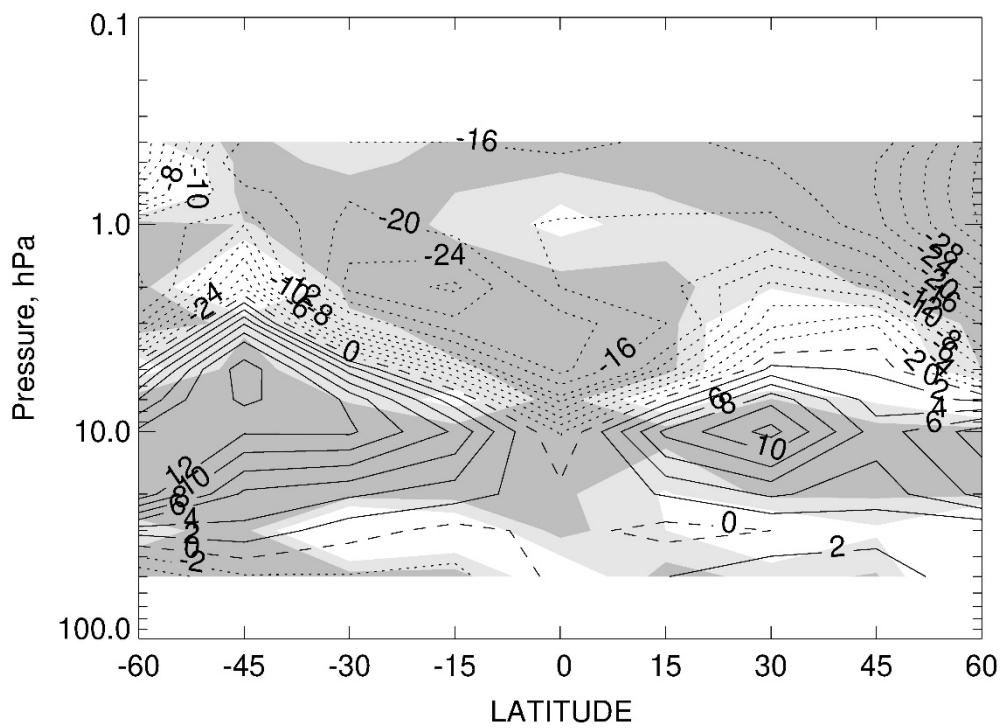
411

412

413

414

415



416

417 Figure 5—As in Fig. 3, but for July 1996 through June 2001.

418

419

420

421

422

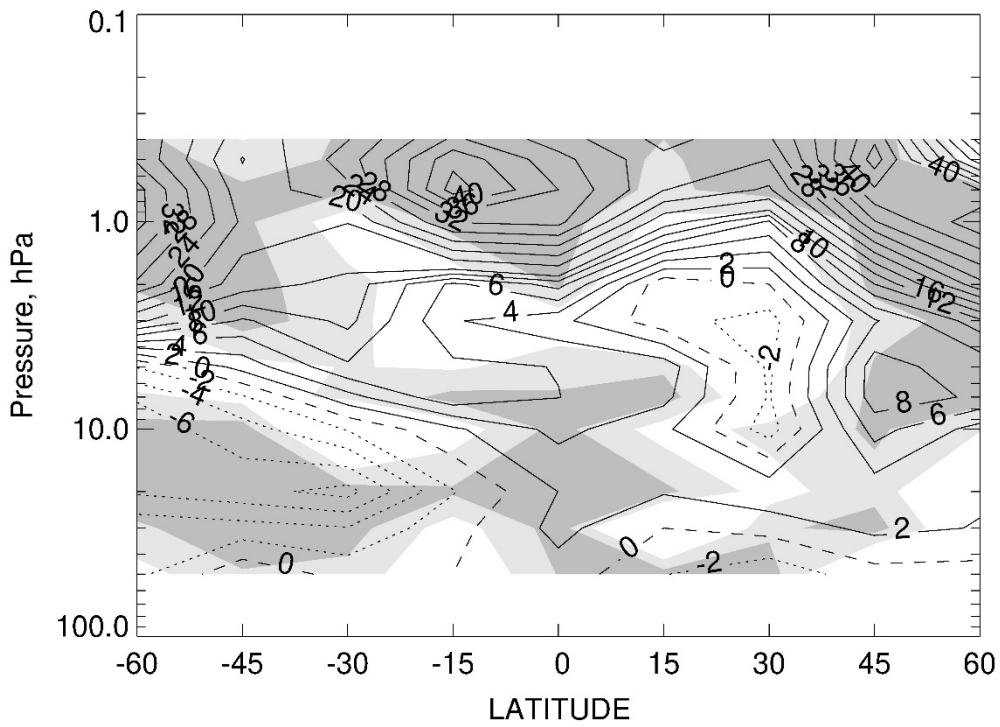
423

424

425

426

427



429

430 Figure 6—As in Fig. 3, but for July 2000 through June 2005.

431

432

433

434

435

436

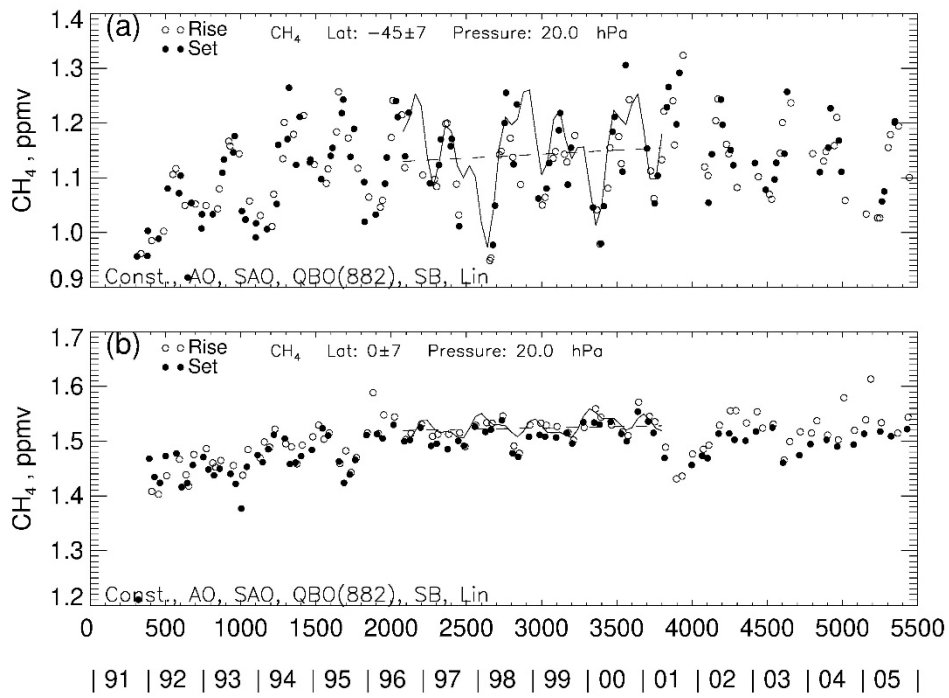
437

438

439

440

441



442

443 Figure 7—As in Fig. 1, but 7(a) is for 45°S and 20 hPa, and 7(b) is for Eq and 20 hPa.

444